

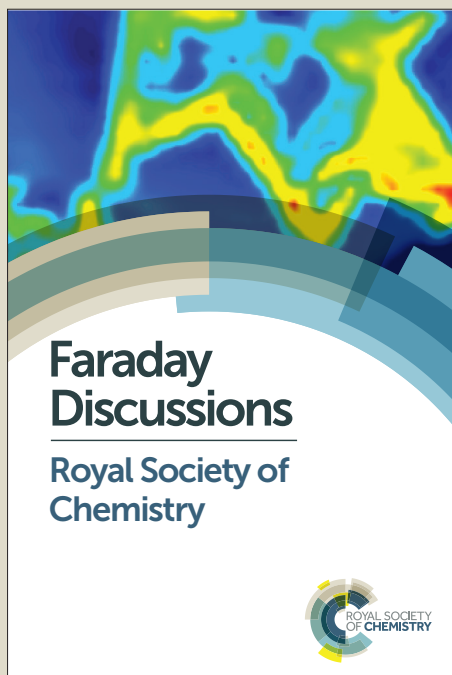
Faraday Discussions

Accepted Manuscript



This manuscript will be presented and discussed at a forthcoming Faraday Discussion meeting. All delegates can contribute to the discussion which will be included in the final volume.

Register now to attend! Full details of all upcoming meetings: <http://rsc.li/fd-upcoming-meetings>



This is an *Accepted Manuscript*, which has been through the Royal Society of Chemistry peer review process and has been accepted for publication.

Accepted Manuscripts are published online shortly after acceptance, before technical editing, formatting and proof reading. Using this free service, authors can make their results available to the community, in citable form, before we publish the edited article. We will replace this *Accepted Manuscript* with the edited and formatted *Advance Article* as soon as it is available.

You can find more information about *Accepted Manuscripts* in the [Information for Authors](#).

Please note that technical editing may introduce minor changes to the text and/or graphics, which may alter content. The journal's standard [Terms & Conditions](#) and the [Ethical guidelines](#) still apply. In no event shall the Royal Society of Chemistry be held responsible for any errors or omissions in this *Accepted Manuscript* or any consequences arising from the use of any information it contains.

X-ray diffraction in temporally and spatially resolved biomolecular science

John R. Helliwell^{a,*}, Alice Brink^{a,b}, Surasak Kaenket^a, Laurina-Victoria Starkey^a and Simon W. M. Tanley^a

5 DOI: 10.1039/b000000x [DO NOT ALTER/DELETE THIS TEXT]

Time-resolved Laue protein crystallography at the ESRF opened up the field of sub-nanosecond protein crystal structure analyses. There are a limited number of such time-resolved studies in the literature. Why is this? The X-ray laser now gives us femtosecond (fs) duration pulses, typically 10 fs up to ~50 fs. Their use is attractive for the fastest time-resolved protein crystallography studies. It has been proposed that single molecules could even be studied with the advantage of being able to measure X-ray diffraction from a ‘crystal lattice free’ single molecule, with or without temporal resolved structural changes. This is altogether very challenging R&D. So as to assist this effort we have undertaken studies of metal clusters that bind to proteins, both ‘fresh’ and after repeated X-ray irradiation to assess their X-ray-photo-dynamics, namely Ta₆Br₁₂, K₂PtI₆ and K₂PtBr₆ bound to a test protein, hen egg white lysozyme. These metal complexes have the major advantage of being very recognisable shapes (pseudo spherical or octahedral) and thereby offer a start to (probably very difficult) single molecule electron density map interpretations, both static and dynamic. A further approach is to investigate the X-ray laser beam diffraction strength of a well scattering nano-cluster; an example from Nature being the iron containing ferritin. Electron crystallography and single particle electron microscopy imaging offers alternatives to X-ray structural studies; our structural studies of crustacyanin, a 320 kDa protein carotenoid complex, can be extended either by electron based techniques or with the X-ray laser representing a fascinating range of options. General outlook remarks concerning X-ray, electron and neutron macromolecular crystallography as well as ‘NMR crystallography’ conclude the article.

30 1 Introduction

The advent of intense synchrotron X-ray sources has allowed time-resolved diffraction in general and macromolecular crystallography in particular to have wide applicability to study time dependent phenomena at the molecular level; as a spearhead time-resolved Laue protein crystallography at the ESRF (<http://www.esrf.eu/UsersAndScience/Experiments/SoftMatter/ID09B>) opened up the field of sub-nanosecond crystal structure analyses.¹ Biomolecular science 'fast time-resolved' examples include carbon monoxy myoglobin and phospho yellow protein (PYP).² More complex cases included following the enzyme reaction of hydroxymethylbilane synthase in the crystal and which are slower by nature.³ There are a limited number of such time-resolved studies in the literature. Why is this? Firstly, crystal lattice interactions can block the necessary structural changes for a given biochemical reaction to proceed. Secondly, crystal size determines a sample's scattering strength and thereby the required exposure time, clearly increasing as a sample gets smaller. The latter obviously can be at odds with the intrinsic time resolution required to monitor a given molecular structural change; different measuring protocols try and ease past this challenge such as the Hadamard measuring sequence⁴ or the simpler approach of crystal to crystal averaging at equivalent time-slices.³ Meanwhile the X-ray laser now gives us femtosecond (fs) duration pulses, typically 10 fs up to ~50 fs.⁵ Their use is attractive for the fastest time-resolved protein crystallography studies. It has been proposed that single molecules could even be studied,⁶ which would free us of the crystal lattice restrictions referred to above. Again though, the sample scattering strength along with the current X-ray laser maximum photons per pulse achievable from the source currently restrict the samples to crystalline arrays albeit micron to submicron ('nano') i.e. small crystal sizes.⁷ In considering these challenges and the clear advantage of being able to measure X-ray diffraction from a single molecule, with or without temporal resolved structural changes, we have studied in detail a class of metal complexes, the platinum hexahalides, as well as the tantalum bromide cluster when bound to hen egg-white lysozyme (HEWL) as a test protein crystal including their 'X-ray-photo-dynamics'.^{8,9} These metal clusters have the major advantage of being very recognisable shapes (octahedral and pseudo spherical). So, where we can expect difficult to interpret electron density maps, and their time-resolved changes in biochemical reactions, these 'marker well-shaped complexes' will offer a start to electron density map interpretations.⁹ A further approach is to investigate the X-ray laser beam diffraction strength of a

well scattering nano-cluster; an example from nature being the iron containing ferritin (which has 2000 iron atoms in ferrihydrite form within a protein multi-subunit shell).¹⁰ Another example would be, in a bionanotechnology approach, an encapsulated metal core within a virus protein shell.

5

2 Understanding the X-ray-photo-dynamics properties of the platinum hexahalides and of the tantalum bromide cluster ($\text{Ta}_6\text{Br}_{12}$) using X-ray crystallography

We have studied in detail a class of metal complexes, the platinum hexahalides, as well as the tantalum bromide cluster when bound to hen egg-white lysozyme (HEWL) as a test protein crystal.^{8,9} Our interest first arose from protein powder X-ray diffraction to exploit the wavelength dependent dispersive differences for phasing of extracted powder diffraction Bragg reflection amplitudes. The larger delta f' signal arising from hexabromide was attractive.⁸ The bromine K edge at 0.92 Å X-ray wavelength was very conveniently placed for two wavelength measurements involving 'on edge' and a remote X-ray wavelength. For the most electron dense cluster of this type however, platinum hexaiodide is more attractive. In ref⁹ we reported the binding behaviour to histidine in HEWL as a test protein. In this paper we report the stability of the platinum hexahalides to prolonged X-ray irradiation. The platinum hexabromide and its photochemical response to UV light has been studied^{11, 12} but not the platinum hexaiodide to our knowledge. These metal clusters have the distinct advantage of being particularly recognisable shapes (octahedral and pseudo spherical). So, where we can expect difficult to interpret electron density maps, and their time-resolved changes in biochemical reactions, these 'marker well-shaped complexes' will offer a start to electron density map interpretations.⁹ The break-up of platinum hexabromide, even when cryocooled, upon prolonged X-ray irradiation, akin to the UV study,¹¹ was reported previously.¹³ Here we report the HEWL with bound PtBr_6 at room temperature also upon prolonged X-ray irradiation.

30

2.1 PtBr_6 , PtI_6 and $\text{Ta}_6\text{Br}_{12}$ heavy atom clusters bound to a protein: their X-ray-photo-dynamics

2.1.1 Crystallisation conditions

HEWL crystals were prepared using the batch method as outlined by Blundell and Johnson (1976),¹⁴ namely: HEWL (60 mg) was dissolved in 0.04 M acetate buffer, pH 4.7 (1 mL) and 10% NaCl (1 mL) was added to the solution. HEWL crystals were then soaked for 24hrs in a solution of either K₂PtBr₆ (10 mM) or K₂PtI₆ (10 mM). A solution of each heavy-atom compound was from a pre-made stock solution of 50 mM in acetate buffer.

In the case of 'HEWL Ta₆Br₁₂ PtBr₆' the protein was co-crystallised with 2 mM Ta₆Br₁₂, forming beautiful green coloured crystals (Figure 1a), of the usual tetragonal HEWL crystal morphology. After being soaked in PtBr₆, the crystals turned from green to the orange colour of the PtBr₆ (Figure 1b). Figure 1c shows the distinctive colour of the 'HEWL soaked in K₂PtI₆' crystals.

2.1.2 X-ray diffraction data collection, protein crystal structure

15 solution and molecular model refinement

For the cryo diffraction data collections, a crystal from each soaking condition was scooped into a loop with paratone used as the cryoprotectant. These X-ray diffraction (XRD) data were measured on a Bruker CCD Pt¹³⁵ home source diffractometer at an X-ray wavelength of 1.5418 Å, carried out at a fixed temperature of 100 K. The XRD data collection strategy used led to a high completeness of unique data, high anomalous differences completeness and data redundancy at a reasonable level. All XRD data were processed using the Bruker software package, PROTEUM 2.¹⁵ We collected repeated X-ray datasets on the same crystal to study the X-ray irradiation on the complexes.

The crystal structures were solved using PHASER_MR¹⁶ and then rigid body and restrained refinement with CCP4i REFMAC5,¹⁷ using the previously reported lysozyme structure 2W1Y as the molecular search model.¹⁸ The use of Phaser_MR was probably not required as 2W1Y is relatively isomorphous with these crystals. Model building, adjustment and refinement were carried out respectively using the COOT molecular graphics programme¹⁹ and REFMAC5 in CCP4i. The crystallographic and molecular model refinement parameters are summarized in the Supplementary foot notes below. All figures were produced using COOT.¹⁹

The experimental conditions for preparing the 'HEWL PtBr₆ room temperature' crystal sample were basically the same as described above namely a native hen egg white lysozyme protein crystal was soaked in 10 mM K₂PtBr₆ for 24 hours. A crystal was selected to be smaller than the X-ray beam size (approx. 0.3mm) but not too small to give too weak a diffraction on an APEXII microfocus sealed tube X-ray source. The crystal was mounted 'wet' in a glass capillary and thereafter remained held at room temperature, approximately 20 C. X-ray diffraction data were recorded over an angular range of rotation of the crystal of 210 degrees by which time i.e. X-ray dose (approximately 2 MGy) the diffraction pattern had noticeably deteriorated. Datasets were grouped according to 30 degree sweeps making seven datasets in all. The high symmetry of the tetragonal lysozyme space group (*P*4₃2₁2) yielded a reasonably good dataset completeness for each 30 degrees sweep of approximately 70%.

2.1.3 Comparison of the X-ray and UV photochemical behaviour of K₂PtBr₆ and conclusions on the X-ray photochemical behaviour of K₂PtI₆ bound to HEWL

2.1.3.1 Cryo experiments

The K₂PtBr₆ with Ta₆Br₁₂ bound in the same crystal allow a direct comparison, side by side as it were, of the two metal complexes. As reported in ref 13 a breakup of the PtBr₆ (Figure 2), occurs versus a stability of the Ta₆Br₁₂ throughout. The other sensitive marker of X-ray irradiation damage is the splitting of the protein disulphides²⁰ and show such an effect for two of the disulphides by a 7th repeat X-ray diffraction data set.

The extension of the cryocrystallographic studies to include the multiple X-ray dataset irradiation stability of the iodo complex (i.e. K₂PtI₆) bound to lysozyme is a natural extension and complements the aim of using these platinum octahedral complexes to facilitate interpreting difficult electron density maps. The first X-ray diffraction dataset electron density (green in Figure 3) and the somewhat diminished (lilac in Figure 3) electron density for PtI₆ at the 6th XRD data set is not as severe as the PtBr₆ break up upon X-ray irradiation. There is a PtI₃ moiety, directly bound to one of the His15 imidazole nitrogens, which is stable versus X-ray dose (i.e. green and lilac electron densities in Figure 3 are identical).

2.1.3.2 Room temperature X-ray crystallographic study of the hen egg white lysozyme with bound PtBr_6 and relation to its chemical kinetics

The X-ray-photo-dynamics behaviour of PtBr_6 at room temperature when bound to hen egg white lysozyme and its stages of stepwise removal of bromine atoms are shown in Figure 4 which compares the metal complex at successive stages of X-ray irradiation namely data sets 1, 3, 5 and 7 (datasets 2, 4 and 6 not shown) i.e. with cumulatively increasing X-ray dose to the same crystal). The occupancies of the Pt and Brs are approximately 0.3; the bound waters that would be expected (see Figure 5) to complete the octahedral arrangement around the platinum centre at 0.3 occupancy are not visible in Figs 4 b to d; this is due to the limited diffraction resolution of 2.2\AA and a diffraction data completeness of $\sim 70\%$ in each case.

The chemical kinetics is basically that of a unimolecular reaction (ie break up) of the platinum hexabromide upon X-ray illumination. Since the X-ray illumination is at a continuous level, simply chosen to allow reasonable strength X-ray diffraction data to be recorded, we cannot determine an absolute rate constant for the break up. We note though that at room temperature the platinum hexabromide break up was more prompt than at cryo temperature in the lysozyme+ PtBr_6 + $\text{Ta}_6\text{Br}_{12}$ study in that the room temperature X-ray diffraction data had to be subdivided into smaller angular portions than for the cryo data. A future experiment could be undertaken whereby a larger X-ray intensity would be used to illuminate a crystal sample eg from an intense synchrotron undulator X-ray beam, which would form an X-ray flash photolysis approach, and then the irradiated sample plunge frozen. This would be repeated with several samples each at different time lapse intervals after X-ray irradiation. Neutron macromolecular crystallography diffraction data sets would then be recorded for each time lapse plunge freeze sample; the neutron beam would then allow the molecular state of the PtBr_6 to be probed without further radiation damage. Of course it would be entirely possible that the break up state would be identical in each neutron derived crystal structure ie if the damage in an intense X-ray beam was ‘instantaneous’. Glebov et al¹¹ in their UV/Vis studies indeed undertook flash photolysis and ‘steady state illumination’ experiments and kinetics analyses and from which we quote:-

“The spectral curves obtained by steady state irradiation and pulse photolysis

coincide, indicating that the first photoaquation step occurred within the time <50 ns.”

3 A short summary of the UV photochemistry of PtBr_6^{2-}

5 The inorganic photophysics of K_2PtBr_6 in aqueous solution under steady state and laser flash photolysis (308 nm) has also been reported on previously¹¹ including a reaction mechanism proposal taking place on a timescale of nanoseconds or shorter involving charge transfer to an excited d-d state for lengthening of the Pt-Br bond distance and subsequent departure of a bromine
10 atom. It is also described that successive steps of bromine removal and take up of a water molecule is possible.

Glebov *et al.*¹¹ reported their experimental results as follows:-

15 *“Photochemistry of the PtBr_6^{2-} complex in aqueous solution was studied by steady state and laser flash photolysis (308 nm). The multistep photo-aquation of the complex occurs in the nano- and micro-second time intervals without the formation of intermediate platinum(III) complexes.”* See their figure reproduced as Figure 5 here. They conclude that *“Thus, experiments with pico- or femto-second time resolution are necessary to perform for detailed investigation of the processes that occur upon the excitation of the PtBr_6^{2-}
20 complex.”*

Our protein single crystal results are consistent with these models showing the successive steps in the removal of bromine atoms in the room temperature PtBr_6 experiment and crystal structure analyses (Figures 4a, b, c and d)

25

4. Specific Conclusions

$\text{Ta}_6\text{Br}_{12}$ is relatively the most stable under repeated X-ray irradiation (Figure 2) with PtI_6 only showing some small changes (Figure 3). Relatively less stable as a heavy

atom complex is the PtBr₆ (Figures 2 and 4).

The study by Glebov *et al.*^{11,12} of PtBr₆ shows that ‘with and without UV/vis light flash’ leads to photo dissociation of the platinum hexabromide (Figure 5). The cryo
5 ‘HEWL Ta₆Br₁₂ PtBr₆’ study (Figure 2) and the room temperature XRD study of
‘HEWL with PtBr₆’ (Figures 4 a - d) concurs with the UV study, all showing a light
induced break-up of the PtBr₆.¹¹ Whilst the UV study of platinum hexaiodide seems
not to have been undertaken, the HEWL PtI₆ behaviour shows that it is relatively
more stable under X-ray irradiation than the PtBr₆ and suggests therefore that the
10 UV stability of PtI₆ would likewise be more stable.

The respective behaviours of the temporal and structural stabilities of these heavy
atom clusters are clearly of interest for a number of reasons. With the femtosecond
XRD ‘diffract before destroy’ method⁵ the X-ray sensitivity of the PtBr₆ is not
15 relevant. However its irradiation by UV light before the X-ray laser diffraction
would prepare an altered oxidation state¹¹ which may be useful. The stability of the
Ta₆Br₁₂ and of the PtI₆ upon prolonged X-ray irradiation is a good property when
synchrotron or home Lab X-ray sources are used for biological crystal structure
determination.

20

5 General Outlook

Whilst our article title is specifically on X-ray diffraction, a more general question is
whether there will be a surge of electron based diffraction techniques for temporally and
spatially resolved molecular science? Electrons interact much more strongly with atoms
25 than do X-rays. Electron crystallography and single particle electron microscopy (EM)
imaging offer alternatives to the trend with X-ray sources such as the X-ray laser for the
study of ever smaller samples. Our X-ray crystal structural studies of the lobster carapace
coloration protein beta-crustacyanin,²¹ have been extended to determine the layout at
around 30 Å resolution of the alpha-crustacyanin complex, a 320 kDa complex of eight
30 beta-crustacyanins,²² using negative stain single particle EM and Small Angle X-ray
Scattering along with ‘rigid body fitting’ of the beta-crustacyanin crystal structure. This
structural study of the alpha-crustacyanin complex can be extended either by electron
based techniques or with the X-ray laser representing a fascinating range of options.²³
The technique of electron single crystal crystallography has very recently gained a major

impetus with successful 3D structural analysis at 2 Å resolution, using molecular replacement, of hen egg white lysozyme as a test protein and using two individual microcrystals.²⁴ It may not be possible to make *de novo*, high resolution, protein structure determinations unless accurate isomorphous derivative intensity differences can be measured.²⁵ However molecular replacement is now the predominant technique in protein crystallography not least due to the fact that the Protein Data Bank contains more and more of the protein folds seen in Nature (the PDB now contains over 100,000 entries). Thus alpha-crustacyanin might yet be solvable with electron (microcrystal) crystallography and using the beta-crustacyanin X-ray crystal structure determined with a xenon heavy atom derivative and softer X-rays from the Daresbury SRS. Clearly there are important general implications for biological crystallography from the electron technique results of ref²⁴ using microcrystals of proteins and complexes of biological macromolecules. Besides static structure determination dynamic studies based on electron crystallography from a microcrystal sample might be easier than from a larger crystal i.e. preserving crystallinity and so on. Again though, like the comment regarding the challenge for electron based techniques of measuring accurate isomorphous heavy atom derivative intensity differences, Bragg reflection intensity changes from temporal structural sequences can be smaller than those induced by a heavy atom and thereby even more difficult to measure precisely. Nevertheless further development of electron crystallography may well open up new options in this fascinating field; Zewail and Thomas have championed the electron based techniques for a general realisation of 4D, space and time, structural studies.²⁶

A regular challenge for X-ray crystal structure analysis of biological macromolecules is the determination of the protonation states of ionisable amino acid side chains of aspartic acid, glutamic acid and histidine. Likewise the orientation of bound water molecules or their state as hydroxyl or hydronium ions is even more challenging. Thus a growing development at the neutron sources are the provision of instruments for neutron macromolecular crystallography notably in Japan at JAERI and JPARC, at the Institut Laue Langevin in Grenoble and at Oak Ridge National Lab, USA on both the research reactor and the SNS. Likewise a variety of the macromolecular crystallographic software analysis packages now provide macromolecular refinement with neutron and X-ray scattering factors. Given the low flux of neutron beams at first sight it would seem that studies of structural and temporal dynamics using neutron macromolecular crystallography would not be

possible. Is this in fact the case? In fact 'No', it is possible with sample freezing to study structural intermediates albeit on a timescale set by the freezing time of the crystal sample.²⁷ This area of neutron macromolecular crystallography is expected to grow; a very recent example is ref ²⁸. One such 'next experiment', as mentioned
5 above, is suggested from consideration of the chemical kinetics of the X-ray induced break up of PtBr₆.

Diffraction based techniques have limits. These have been highlighted in the recent book on NMR crystallography,²⁹ which I reviewed.³⁰ Quoting from Chapter 1 of this book:- "*A
10 key advantage is the case of host-guest complexes where the guest is mobile and obviously thereby disordered and its visibility absent or limited in the diffraction-derived structural analyses....(thus)....diffraction-based information forms an important background to investigations and where NMR is essential to delineate motional effects'....NMR measurements are 'in addition to the relaxation times
15 information which extends down to the microseconds region'.There are two major areas in which complementary information (to diffraction) is desirable: Molecular-level mobility and purely spatial, i.e. static, disorder'.*" Chapter 27 of the book³¹ is devoted to structural biology and included NMR measurements by Martin and Zilm of a protein, ubiquitin (consisting of 76 amino acids and which has a molecular mass of about 8.5
20 kDa), in three different sample states "of microcrystals, nanocrystals and lyophilized (i.e. amorphous)". The solid state NMR spectra for the nanocrystals of ubiquitin were equivalent to the spectra from the larger crystals; the difference was in the amorphous solid state ubiquitin spectra. As macromolecular crystallographers we tend not to worry too much about the sample state details and yet the properties of metallic nanoparticles,
25 for example, are known to be different from bulk solids. This is an interesting further question for debate as the diffraction methods take macromolecular crystallography into the nanocrystal sample size domain.

5. Acknowledgements

30 We are grateful to the University of Manchester for general support, to the EPSRC for a PhD studentship to SWMT, to the Thailand Government for studentship support to SK, to the SASOL Young Academic Collaboration Initiative for Dr Alice Brink, to the School of Chemistry for crystallization and computing facilities and to the Faculty of Life Sciences for X-ray diffraction facilities. We are very grateful to Dr Colin Levy and
35 Dr Pat Bryant for their excellent stewardship of the Manchester Institute of Biotechnology ('MIB') X-ray Facility.

^a School of Chemistry, University of Manchester M13 9PL, UK. Tel: 441612754970; E-mail: john.helliwell@manchester.ac.uk

^b Department of Chemistry, University of the Free State, Bloemfontein 9300, South Africa. E-mail: alice.brink@gmail.com

5 † Electronic Supplementary Information (ESI) available: Figures 2, 3 and 4 were calculated using Refmac5 (Main text ref ¹⁷) using Hen Egg White Lysozyme coordinates PDB code 2W1Y (Main text ref ¹⁸). The CCP4 mtz format processed structure factor amplitudes ‘X-ray radiation damaged’ diffraction data files used to make the figures 2, 3 and 4, displayed with COOT (Main text ref ¹⁹), are provided as Supplementary files to this paper. The cumulative absorbed X-ray dose by the time of
10 the final datasets in the cryo cases was approximately 10 MGy and in the room temperature case approximately 2MGy; uncertainties in these numbers arise from the X-ray generator flux at the sample being an estimate and the chemical composition of the protein crystal irradiated in each case is also somewhat approximate due to the inherent uncertainty in the bound atom occupancies and the chemical composition finally of the protein crystal solvent channels. A detailed examination of such
15 X-ray dose estimates can be found in Main text ref ³². Nevertheless the cumulative X-ray dose given is a good guide to the dose absorbed by the crystal samples. An absorbed X-ray dose of 30 MGy was recommended by Owen *et al.* 2006 (Main text ref ³³) as an appropriate dose limit for typical macromolecular crystallography experiments conducted with the sample held at cryo temperatures i.e. typically 100 K; these cryo data collection experiments reported here are well within that
20 absorbed X-ray dose limit as is also evident by the good quality of the protein electron density even at the final repeat X-ray diffraction dataset with the exception of some disulphide bridge splitting.

‡ Figures 2, 3, 4: HEWL crystal space group in each case was $P4_32_12$; the electron density maps displayed in Figures 2, 3 and 4 were respectively calculated at 1.7Å, 1.6Å and 2.2 Å. The PDB codes for the previously published ‘HEWL PtBr₆’ and ‘HEWL PtI₆’ X-ray crystal structures
25 determined at 100 K (ref ⁹) are respectively 4OWH and 4OWC. The PDB code for the ‘HEWL Ta₆Br₁₂ PtBr₆’ crystal structure determined at 100 K described for the first time here is 4R6C. Full details of the XRD data sets and molecular model parameters for these metal atom complexes bound to the HEWL protein can be found in these PDB files.

References

5

- ¹ J. R. Helliwell and P. M. Rentzepis, Editors. *Time-Resolved Diffraction*, Oxford University Press, 1997; D. W. J. Cruickshank, J. R. Helliwell and L.N. Johnson, Editors *Time-resolved Macromolecular Crystallography* Oxford Science Publications
- ² Z. Ren, D. Bourgeois, J. R. Helliwell, K. Moffat, V. Strajer and B. L. Stoddard, *J. Synchrotron Rad.*, 1999, **6**, 891–917
- ³ J. R. Helliwell, Y. P. Nieh, J. Raftery, A. Cassetta, J. Habash, P. D. Carr, T. Ursby, M. Wulff, A.W. Thompson, A. C. Niemann and A. Hädener, *Faraday Trans.*, 1998, **94**, 2615–2622.
- ⁴ B. A. Yorke, G. S. Beddard, R. L. Owen and A. R. Pearson *Nature Methods* (2014) (DOI: 10.1038/nmeth.3139; URL:<http://dx.doi.org/10.1038/nmeth.3139>)

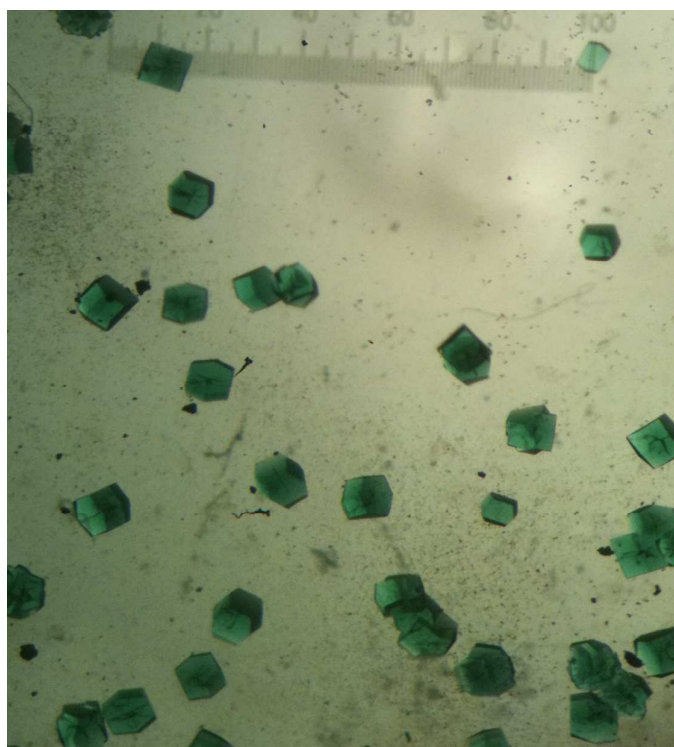
- ⁵ J. C. H. Spence and H. N. Chapman, Editors. *Biology with free-electron X-ray lasers*. *Phil. Trans. R. Soc. B*, 2014, **369**, p. 1647
- ⁶ R. Neutze, R. Wouts, D. van der Spoel, E. Weckert and J. Hajdu, *Nature*, 2000, **406**, 752-757.
- ⁷ J. R. Helliwell, *Science*, 2013, **339**, 146-147
- ⁸ J. R. Helliwell, A. M. T. Bell, P. Bryant, S. J. Fisher, J. Habash, M. Helliwell, I. Margiolaki, S. Kaenket, Y. Watier, J. Wright and S. Yalamanchilli, *Z. Krist.*, 2010, **225**, 570-575.
- ⁹ S. W. M. Tanley, L-V. Starkey, L. Lamplough, S. Kaenket and J. R. Helliwell, *Acta Cryst. F*, 2014, 1132-1134.
- ¹⁰ J. M. A. Smith, J. R. Helliwell and M. Z. Papiz, *Inorg. Chim. Acta*, 1985, **106**, 193-196.
- ¹¹ E. M. Glebov, V. F. Plyusnin, V. P. Grivin, A. B. Venediktov and S. V. Korenev, *Russ. Chem. Bull., Int. Ed.*, 2007, **56**, 2357-2363.
- ¹² V. Balzani and V. Carassiti, *J. Phys. Chem.*, 1968, **72**, 383-388.
- ¹³ J. R. Helliwell, S. Kaenket, C. Levy, P. Bryant, L. Lamplough, J. Raftery, L-V. Starkey, E. Kotsiliti, I. Margiolaki, A. Fitch and J. P. Wright, *Reported at 7th Radiation Damage 'RD7' Conference*, 2012, held Diamond Light Source, Harwell Science and Innovation Campus, Oxfordshire, UK.
- ¹⁴ T. L. Blundell, L. N. Johnson, *Protein Crystallography*, 1976, pp. 66-77. New York: Academic Press.
- ¹⁵ Bruker, PROTEUM2. Version 2. 2006, Bruker AXS Inc., Madison, Wisconsin, USA.
- ¹⁶ A. J. McCoy, R. W. Grosse-Kunstleve, P. D. Adams, M. D. Winn, L. C. Storoni and R. J. Read, *J. Appl. Cryst.*, 2007, **40**, 658-674.
- ¹⁷ G. N. Murshudov, P. Skubák, A. A. Lebedev, N. S. Pannu, R. A. Steiner, R. A. Nicholls, M. D. Winn, F. Long and A. A. Vagin, *Acta Crystallogr.*, 2011, **D67**, 355-367
- ¹⁸ M. Cianci, J. R. Helliwell, and A. Suzuki, *Acta Cryst.*, 2008, **D64**, 1196-1209.
- ¹⁹ P. Emsley, and K. Cowtan, *Acta Cryst.*, 2004, **D60**, 2126-2132.
- ²⁰ J. R. Helliwell, *J. Crystal Growth*, 1988, **90**, 259-272.
- ²¹ M. Cianci, P. J. Rizkallah, A. Olczak, J. Raftery, N. E. Chayen, P. F. Zagalsky and J. R. Helliwell, *PNAS*, 2002, **99**, 9795-9800.
- ²² N. H. Rhys, M.-C. Wang, T. A. Jowitt, J. R. Helliwell, J. G. Grossmann and C. Baldock, *J. Synchrotron Rad.*, 2011, **18**, 79-83
- ²³ J. R. Helliwell, *Crystallography Reviews*, 2010, **16**, 231-242.
- ²⁴ B. L. Nannenga, D. Shi, A. G. W. Leslie and T. Gonen, *Nature Methods*, 2014, doi:10.1038/nmeth.3043
- ²⁵ M. E. Dumont, J. W. Wiggins and S. B. Hayward, *Proc. Natl. Acad. Sci. USA*, 1981, **78**, 2947-2951
- ²⁶ A. Zewail and J. M. Thomas, *4D Electron Microscopy: Imaging in Space and Time*, Imperial College Press, London, 2010.
- ²⁷ M. P. Blakeley, A. J. Kalb (Gilboa), J. R. Helliwell and D. A. A. Myles, *Proc. Natl. Acad. Sci. USA*, 2004, **101**, 16405-16410.
- ²⁸ C. M. Casadei, A. Gumiero, C. L. Metcalfe, E. J. Murphy, J. Basran, M. G. Concilio, S. C. M. Teixeira, T. E. Schrader, A. J. Fielding, A. Ostermann, M. P. Blakeley, E. L. Raven and P. C. E. Moody, *Science*, 2014, doi: 10.1126/science.1254398
- ²⁹ R. K Harris, R. E. Wasylshen and M. J. Duer, Editors. *NMR Crystallography*, John Wiley & Sons, Ltd., Chichester, 2009.
- ³⁰ J. R. Helliwell, *Crystallography Reviews*, 2014, **18**, 241-245.
- ³¹ D. Middleton, Chapter 27 in *NMR Crystallography*, edited by R. K Harris, R. E. Wasylshen and M. J. Duer, John Wiley & Sons, Ltd., Chichester, 2009; and see specifically R.W. Martin and K. W. Zilm, *J Magnetic Resonance*, 2003, **165**, 162-174.
- ³² J. R. Helliwell and S. W. M. Tanley, *Acta Cryst.*, 2013, **D69**, 121-125
- ³³ R. L. Owen, E. Rudino-Pinera and E. F. Garman, *PNAS USA*, 2006, **103**, 4912-4917

X-ray diffraction in temporally and spatially resolved biomolecular science

John R. Helliwell^{a,*}, Alice Brink^{a,b}, Surasak Kaenket^a, Laurina-Victoria Starkey^a and Simon W. M. Tanley^a

Figures:

Figure 1, Lysozyme crystals cocrystallized with $\text{Ta}_6\text{Br}_{12}$ (*a.* top) and soaked with K_2PtBr_6 (*b.* middle); the orange of PtBr_6 beats the green of $\text{Ta}_6\text{Br}_{12}$ and finally (*c.* bottom) HEWL crystals soaked in K_2Pt_6 .



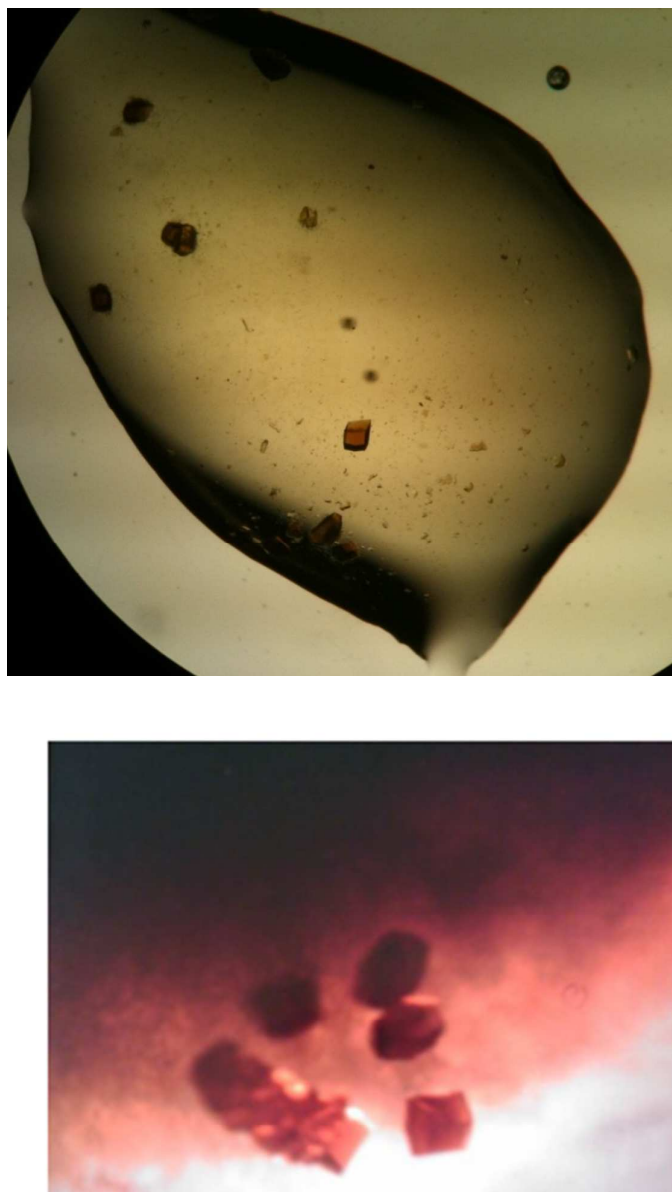


Figure 2. The comparison of the XRD stability behaviour of $\text{Ta}_6\text{Br}_{12}$, which is stable, versus PtBr_6 and its clear break up as evidenced by X-ray data set 0 (electron density difference map contoured at 3 sigma green) and data set 6 (electron density difference map contoured at 3 sigma lilac). The nearest amino acid residue to the PtBr_6 complex, which is Arg 14, is labelled; note the nice octahedral electron density for the first X-ray diffraction dataset (green) and the essentially absent lilac density for it at the 6th data set. At the lower portion of the figure the equivalent green and lilac electron densities are for the $\text{Ta}_6\text{Br}_{12}$ moieties, there are two of them, and whose stabilities to the X-rays, which is very good, are essentially identical. The protein model is 2W1Y and the maps are each rigid body 2W1Y model refinement Fo-Fc 'omit' (ie neither $\text{Ta}_6\text{Br}_{12}$ or PtBr_6 are included in the model) electron density difference maps.

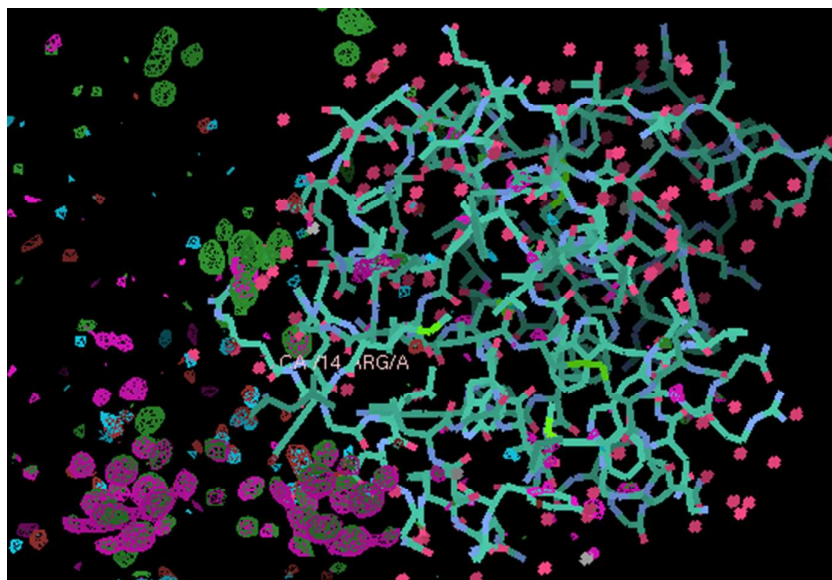


Figure 3. The comparison of the XRD stability behaviour of PtI_6 and PtI_3X ; comparison of data set 0 (electron density difference map contoured at 3 sigma green) and data set 6 (electron density difference map contoured at 3 sigma lilac). The nearest amino acid residue to both moieties, His15, is labelled; note the nice octahedral electron density for PtI_6 (right, green; viewed down the three fold axis of symmetry of the octahedron). The first X-ray diffraction dataset electron density (green) and the somewhat diminished lilac electron density for PtI_6 at the 6th XRD data set (but not as severe as the PtBr_6 break up upon X-ray irradiation). The PtI_3X moiety, directly bound to one of the His15 imidazole nitrogen, is stable versus X-ray dose (i.e. green and lilac electron densities are identical). The refined structure of HEWL PtI_6 data set 0 PDB code is 4owc (ref 9). The protein model shown here is 2W1Y and the maps are each rigid body 2W1Y model refinement Fo-Fc 'omit' (ie neither the PtI_6 or the PtI_3X are included in the model) electron density difference maps.

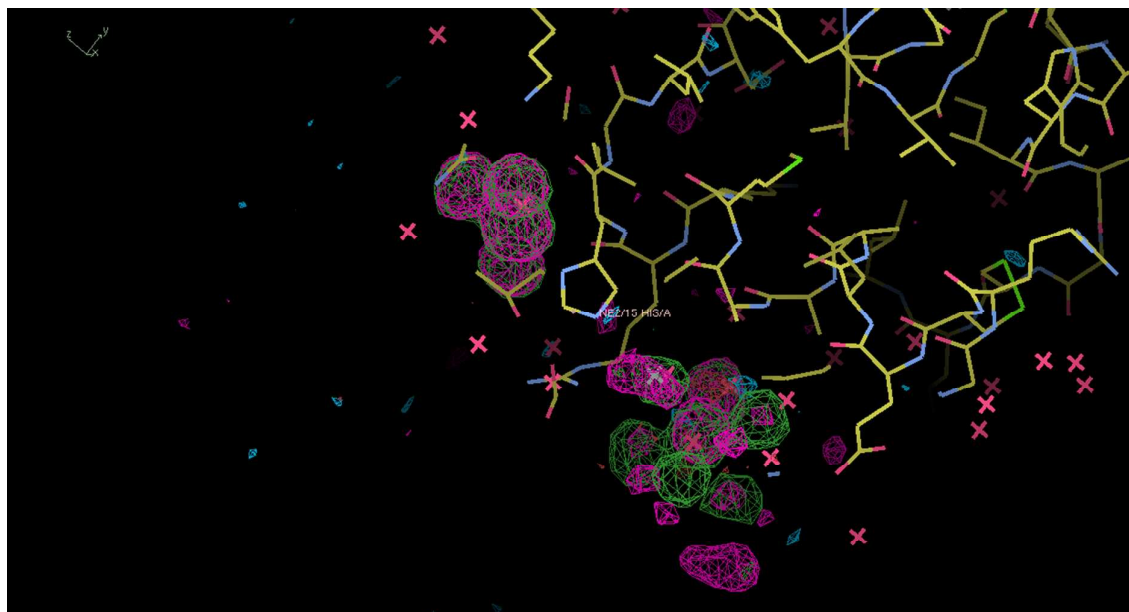
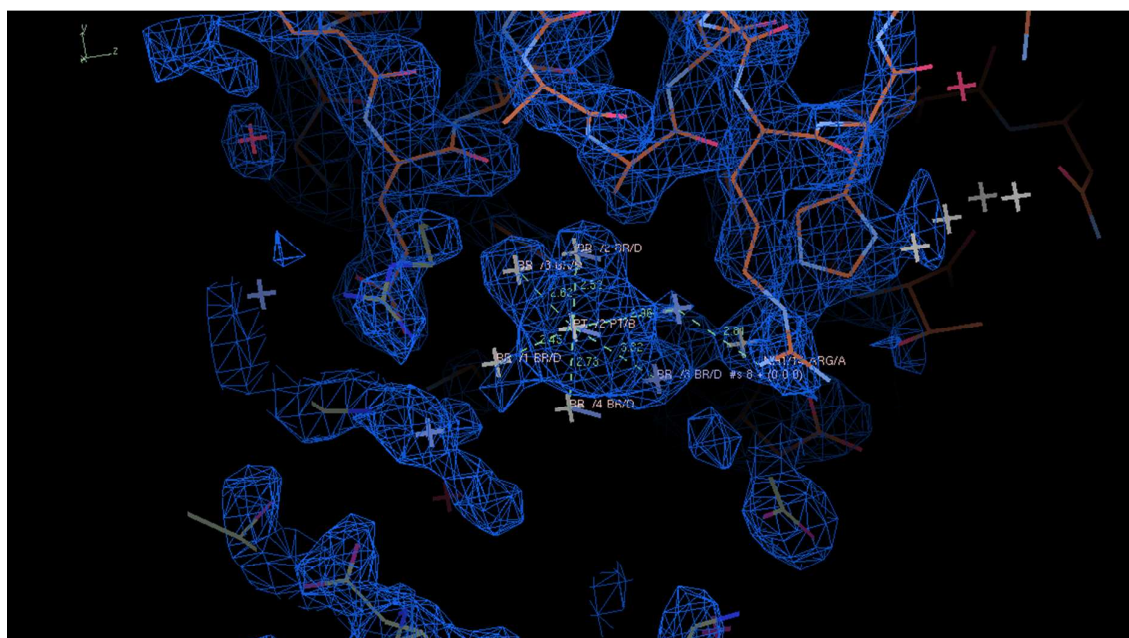
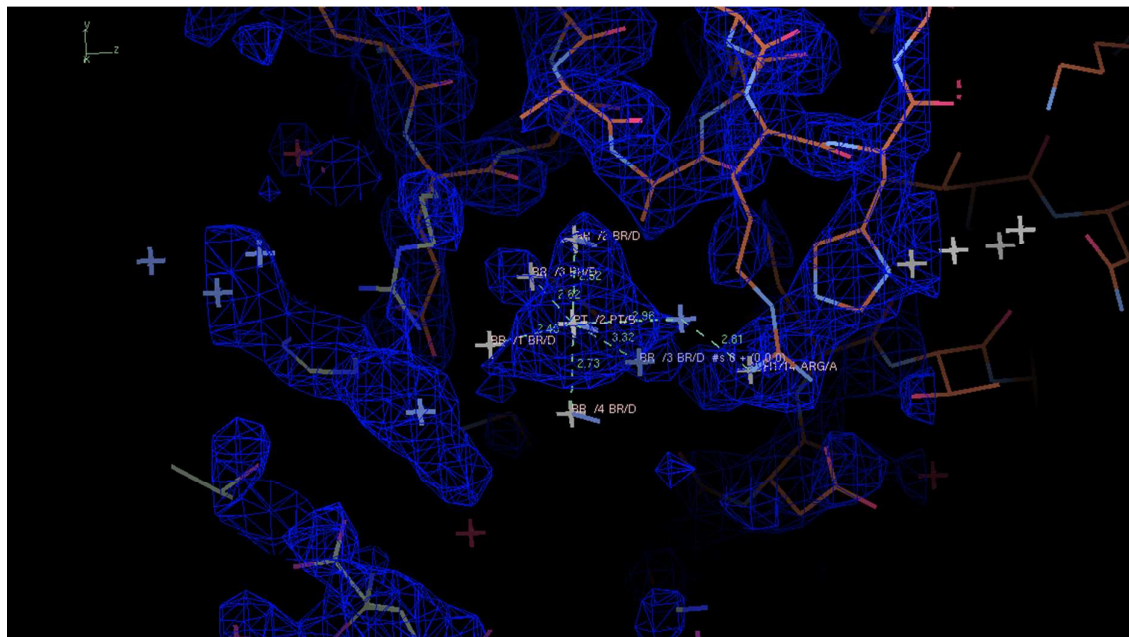


Figure 4 The X-ray-photo-dynamics behaviour of PtBr_6 at room temperature when bound to hen egg white lysozyme and its stages of stepwise removal of bromine atoms evidenced by a comparison of (a) data set 1 (b) data set 3 (c) dataset 5 and (d) dataset 7. Datasets 1 through to 7 are with cumulatively increasing X-ray dose to the same crystal. The nearest amino acid residue to the PtBr_6 complex is Arg 14, which is on the right hand side of the platinum complex and labelled. The protein model is the restrained refined 'HEWL_PtBr6 RT dataset 1' and the electron density difference maps in blue are each rigid body 2W1Y model refinement 2Fo-Fc 'omit' maps ie PtBr_6 not included in the model (1.4rms contour level). The occupancies of the Pt and Brs are approximately 0.3; the bound waters that would be expected (see Figure 5) to complete the octahedral arrangement around the platinum centre at 0.3 occupancy are not visible in Figs 4 b to d; this is due to the limited diffraction resolution of 2.2\AA and diffraction data completeness of $\sim 70\%$ in each case.

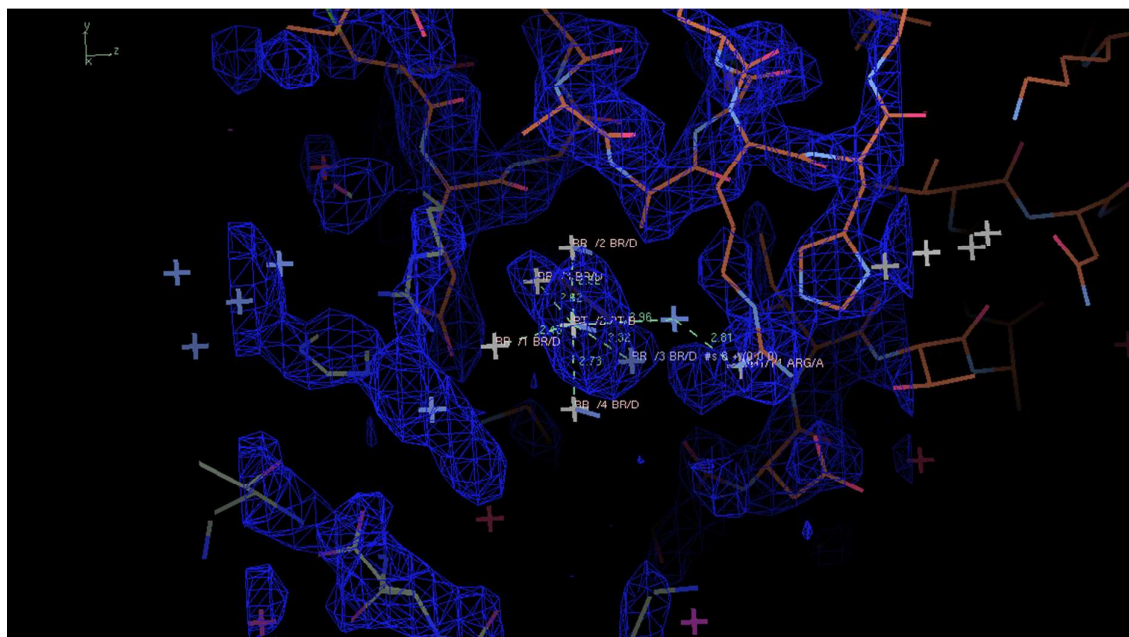
(a)



(b)



(c)



(d)

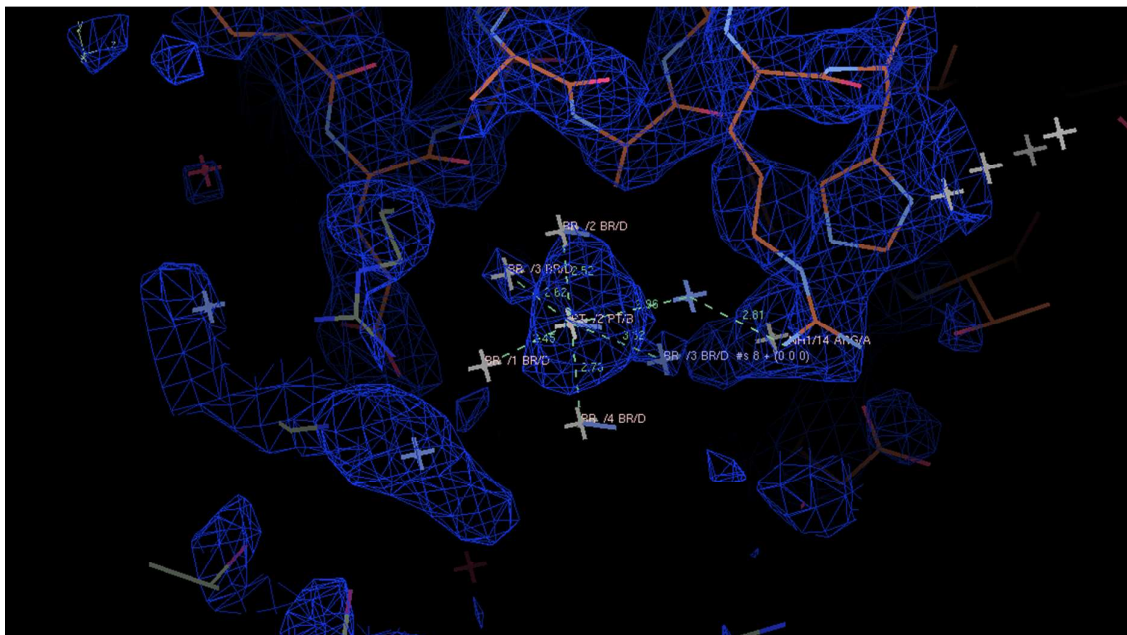


Figure 5. Glebov *et al.*¹¹ reported results as follows:- “Photochemistry of the PtBr_6^{2-} complex in aqueous solution was studied by steady state and laser flash photolysis (308 nm). The multistep photo-aquation of the complex occurs in the nano- and micro-second time intervals without the formation of intermediate platinum(III) complexes.”

